A Sensor Architecture for the Robotic Control of Large Flexible Space Structures

Amy Bilton*, Yoshiyuki Ishijima**, Matthew Lichter*, and Steven Dubowsky*

*Department of Mechanical Engineering
Massachusetts Institute of Technology
Cambridge, MA, USA
bilton@alum.mit.edu, {lichter|dubowsky}@mit.edu

**Japan Aerospace Exploration Agency
Guidance, Controls, and Dynamics Group
Tsukuba, Ibaraki, Japan
ishijima.yoshiyuki@jaxa.jp

Abstract - The future construction and maintenance of very large space structures (LSS) such as orbital solar power stations and telescopes will require teams of free-flying space robots. For robots to effectively perform these tasks, they will require knowledge of the structure's vibrations. Here, a robotic based sensor architecture for the vibration estimation of very large structures is presented. It is shown that this information can be effectively estimated by combining data provided by free-flying remote robot "observers" with range sensors with structure-mounted acceleration sensors. A modified Kalman filter fuses low-bandwidth vision data from the remote sensing robots with the high-bandwidth, but spatially sparse structure-mounted acceleration sensors. Results from experimental studies are presented that confirm the effectiveness of this approach.

Index Terms – space structures, cooperative sensing, shape estimation, space robotics, Kalman filter

I. INTRODUCTION

Very large space structures will be required for such future applications as space solar power plants and space telescopes. These structures will need to be constructed on-orbit. Due to the risks and costs of human extravehicular activity, teams of robots will be essential for such construction [1,2], see Fig 1.

One scenario of LSS construction would consist of three phases. In the first phase, LSS substructure modules are deployed from a launch vehicle. These modules are then maneuvered to the close proximity of the main LSS by a team of free-flying robots. Finally, the module is assembled into the main LSS by a team of manipulators likely mounted on the LSS itself [2].

There are a number of technical challenges associated with such robotic construction. Space structures need to be made of lightweight materials and will be highly flexible with very low damping and natural frequencies. It is important that vibrations be controlled during the structure's transportation and assembly in order to prevent damage to both the structure and the robots. Measurements of vibrational motions of the flexible structure are essential to the performance of transportation and assembly controllers [3,4]. In this paper an architecture is presented that uses available data from structure-mounted sensors and free-flying robot observers to provide an accurate estimate of the structure's shape. This allows the structure to be manipulated by other robots with minimal vibration.

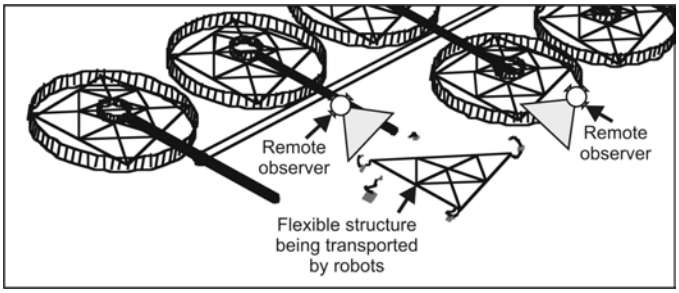

Fig 1. In-orbit construction of LSS by cooperative robots.

Estimating the vibrations of a flexible structure is difficult and has been a topic of much research. Chen used a Kalman filter to simultaneously estimate the shape of a flexible structure and identify the structure parameters, although this approach did not consider sensor limitations [5]. Many researchers have examined the use of on-board sensors, such as accelerometers, strain gauges, etc., to estimate the modal parameters [6,7,8,9]. These sensors provide measurements at

high frequencies, but can only be located at discrete points along the structure. Hence, structure-mounted sensors have low spatial frequency. A large number of accelerometers may be required to accurately estimate the shape of a vibrating structure. Such a large sensor array would require extensive and complex cabling, power supplies, electronics, etc. that would increase cost and weight and reduce reliability. In addition, structure mounted sensors cannot measure the free-rigid body motions of the structure.

The use of range image sequences has also been considered as a method of estimating the shape of a LSS [10,11,12]. Vision sensors placed on free-flying robot observers (laser range finders, stereo cameras, etc.) can capture dense spatial deflection information for the flexible space structure, but their temporal bandwidth is limited. Also, range images are noisy, and data may be missing from large regions due to obfuscation. The harsh lighting conditions of space are often a problem for many vision sensors.

Here the advantages of each sensor type (structure-mounted and mobile-robot based) are exploited by using them in concert. The high spatial resolution provided by the vision system is complementary to the high temporal resolution provided by the structure-mounted sensors. In this approach, the low-frequency vision data is fused with high-frequency acceleration measurements in a nonlinear Kalman filter to provide an estimate of the modal coefficients. These estimates can then be used by control robots to minimize the vibrations of a LSS during construction.

The placement of the vision and structure-mounted sensors can affect the performance of this estimator. In this work, the structure-mounted accelerometers are placed in order to maximize the observability of the vibration using the D-Optimality criteria [13]. Research has also been conducted to determine the optimal placement and number of remote-observer robots, for details refer to [11,14].

It is shown that this architecture provides an accurate shape estimate when experimentally tested using emulated space hardware. The architecture is compared with the results obtained when using estimates based solely on acceleration or vision measurements. Results show that the vision and acceleration-based estimator performs very well. It is able to meet the performance specifications with a limited number of on-board acceleration sensors and relatively low vision system sample rate. Using only a one type of sensor requires excessive demands on the single sensor suite.

II. The Decoupled Controller

This fused estimation approach can be used to provide real-time feedback to control robots. Large space structure transportation is one task where the feedback of modal coefficients could be utilized to improve performance. Fig. 2 schematically shows a large flexible space structure being transported by two robots equipped with thrusters and manipulators. Estimates of the modal coefficients are provided to the transportation robots by fusing information from structure-mounted accelerometers and remote-vision sensors on global-observer robots.

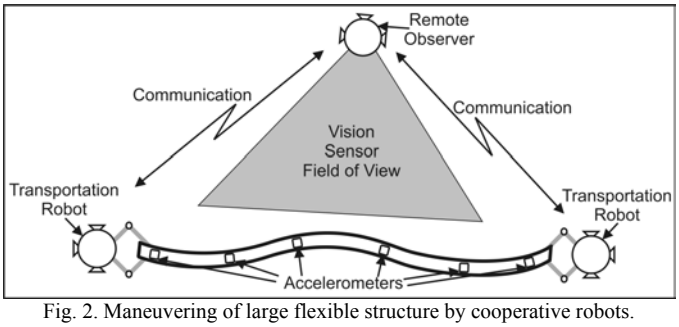

Fig. 2. Maneuvering of large flexible structure by cooperative robots.

The decoupled controller developed in [3] is shown in Fig. 3. For details of this algorithm, please refer to [3]. This is just one of a number of robot controllers used to control the vibrations of flexible structures [15,16]. All such controllers require knowledge of the structure's vibration. This estimation algorithm could also be used in terrestrial applications such as cranes or other construction equipment [17].

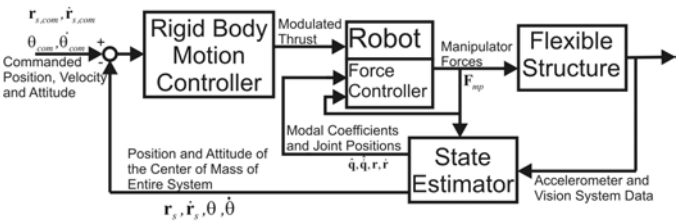

Fig. 3. Control architecture [3].

The performance of the decoupled controller was compared in simulation to a PD-controller where the robot acts as a mass-spring-damper to passively damp-out the structural vibrations. In this case, the algorithm does not require knowledge of the beam vibrations. Fig. 4 shows a simulated slew maneuver, in which two 100 kg robots grasp either end of a 200 m long flexible structure. The robots transport the center of the beam 150 m in the X and Y direction while rotating the structure by 90 degrees. The objective is to transport the structure to its pre-assembly position while exciting minimal vibration, to prevent damage to the module and robots. The details of the simulation parameters can be found in Table 1.

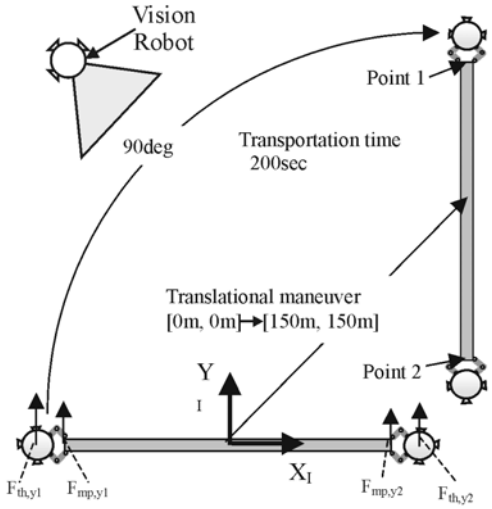

Fig. 4. Transportation manuever using a team of robots.

TABLE 1
SIMULATION PARAMETERS

Parameters	Values
Flexible Structure	Mass m_b :600kg, Length L : 200m, Inertia I_{zz} : 2×10^6 kgm^2 Natural frequencies without robots: 0.20, 0.55, 1.08, 1.78, 2.67, 3.75, 5.02Hz (seven modes considered) Flexural Rigidity (EI): 13×10^6 Nm^2
Robot	Mass m_r:100kg
Thrusters	Thrust F_{max} : ±20N or 0 N (X_G, Y_G direction) Minimum ON/OFF time : 50msec Response Delay: 50msec
Manipulators	Length:1m + 1m (2-DOF)
Accelerometers	Sample Rate:100 Hz Sensor Noise: σ_a=0.1 m/s^2
Vision Sensors	Sensor Noise: σ_v=0.5 m

Fig. 5 shows the end deflection during the maneuver for the case when the robots do not have sensory measurements of the flexible modules vibration. Hence, the manipulators can only provide passive damping to control the vibrations in the structural module. The module undergoes significant vibrations during the transportation manuever. In addition, the vibrations take a long time to dissipate.

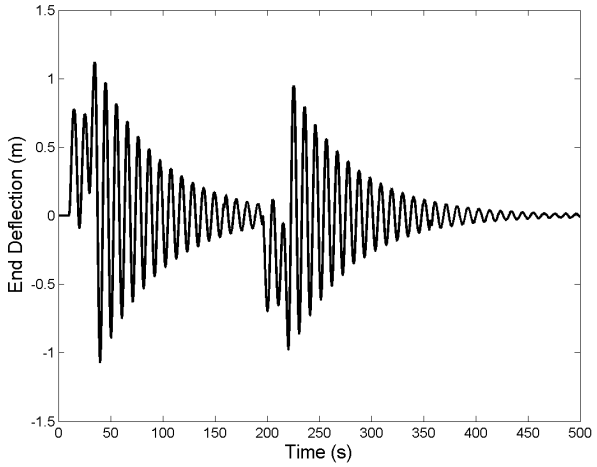

Fig. 5. End deflection of beam during maneuver - without vibration measurements.

Fig. 6 shows the end deflection of the structure when using the decoupled controller developed in [3] that uses knowledge of the beam vibration. This case used an estimate obtained from 7 structure-mounted accelerometers and 2 Hz vision data. The decoupled controller has decreased the maximum deflection during the manuever to 0.4m. Also, the residual vibration following the manuever is very small (less than 2cm peak-to-peak). Using the knowledge of the modal coefficients has greatly improved the performance of the system.

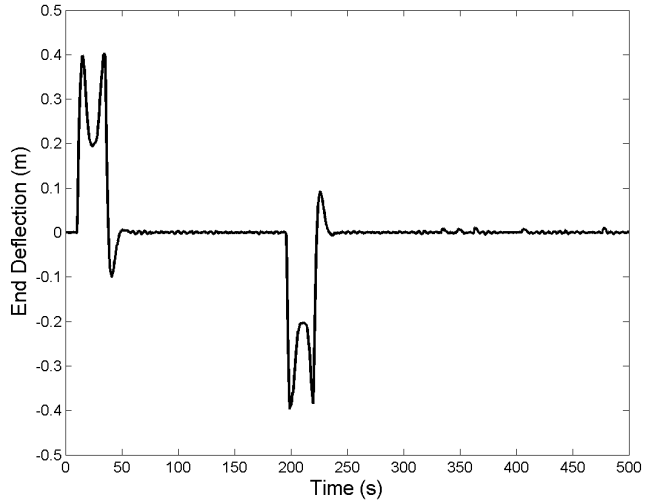

Fig. 6 End deflection of beam during maneuver – with vibration measurements.

III. Analytical Development

A. Assumptions

The sensors in this problem are assumed to provide data at synchronous intervals and communication delays are assumed to be negligible. The sensor noise is assumed to be additive, white, and unbiased, but not necessarily Gaussian. It is also assumed that the mode shapes are known only approximately. These can be found using finite element analysis or on ground testing. The initial uncertainty of the modal damping and frequencies is assumed to be less than 20%.

B. Estimation Structure

For a linear-elastic system, the deformation of the structure, which will be measured by the range imagers, can be written as:

$$z(x,t) = \sum_{i=1}^{m} q_i(t)\phi_i(x) = \mathbf{q}(t)^T \mathbf{\Phi}(x) \tag{1}$$

where $\phi_i(x)$ is the i^{th} mode shape of the structure, m is the number of excited modes, and $q_i(t)$ is the magnitude of the i^{th} modal coefficient. The acceleration of points on the structure can be written as:

$$\ddot{z}(x,t) = \sum_{i=1}^{m} \ddot{q}_i(t)\phi_i(x) = \ddot{\mathbf{q}}(t)^T \mathbf{\Phi}(x) \tag{2}$$

where the dynamics of $q(t)$ are given by:

$$\ddot{q}_i(t) = b_{mi}F(t) - \omega_i^2 q_i(t) - 2\zeta_i\omega_i\dot{q}_i(t) \tag{3}$$

where b_i is the magnitude of the mode shape ϕ_i at the position of the robot, $F(t)$ are the forces applied by the robot to the structure, ω_i is the i^{th} modal frequency and, ζ_i is the i^{th} modal damping coefficient.

The objective is to estimate the $q_i(t)$ and $\dot{q}_i(t)$ of the modes of interest and provide these values to the controller. Using the values of $q_i(t)$ also allows us to obtain an estimate of the shape of the structure using simple modal reconstruction.

The estimation architecture is shown in Fig. 7. The estimation occurs in three steps. First, the vision data is condensed in a modal decomposition that results in coarse estimates of modal coefficients, $\breve{q}_i(t)$. In the second step, the coarse estimates of the modal coefficients obtained from vision data are merged with the accelerometer measurements in a multi-rate nonlinear Kalman filter, resulting in a refined estimate of the modal coefficients, $\hat{q}_i(t)$. In the final step, the estimated modal coefficients are combined with the mode shapes to give the structure a final shape. This section will now detail these steps.

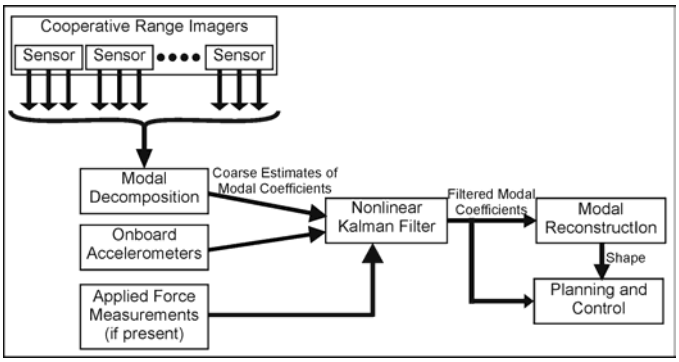

Fig. 7. Estimation architecture.

C. Modal Decomposition

The modal decomposition of vision data is outlined below, details can be found in [14]. Here only the key equations are highlighted. Using the vision data, a coarse estimate of the modal coefficient is produced by:

$$\breve{\mathbf{q}}(t) = \mathbf{M}_y^{-1}\left\langle \Phi, \bar{z} \right\rangle_y = \mathbf{q}(t) + \mathbf{M}_y^{-1}\left\langle \mathbf{\Phi}, \mathbf{e}_v \right\rangle_y = \mathbf{q}(t) + \mathbf{w} \tag{4}$$

where $\mathbf{M}_y$ is the modal correlation matrix, $\mathbf{\Phi}$ is a matrix whose columns are composed of the mode shapes of the structure, $\mathbf{e}_v$ is the vision measurement noise vector, the vector is the measured deformation of the flexible structure, and $\mathbf{w}_v$ is the resultant noise on the coarse estimate. The covariance of $\breve{\mathbf{q}}(t)$ is given by:

$$\mathbf{\Lambda}_{w_v w_v} = \sigma_{e_v}^2 \mathbf{M}_y^{-1} \tag{5}$$

where $\sigma_{e_v}^2$ is the variance on the vision measurements. Note that is the variance is not uniform for all sensors an alternate form of (6) is needed. The covariance for this case can still be easily computed, for details refer to [11].

Acceleration measurements are given by:

$$\begin{Bmatrix} \ddot{\bar{z}}(x_1,t) \\ \vdots \\ \ddot{\bar{z}}(x_i,t) \\ \vdots \\ \ddot{\bar{z}}(x_n,t) \end{Bmatrix} = \begin{Bmatrix} \ddot{z}(x_1,t) \\ \vdots \\ \ddot{z}(x_i,t) \\ \vdots \\ \ddot{z}(x_n,t) \end{Bmatrix} + \begin{Bmatrix} e_1 \\ \vdots \\ e_i \\ \vdots \\ e_n \end{Bmatrix} \Leftrightarrow \ddot{\bar{\mathbf{z}}} = \ddot{\mathbf{z}} + \mathbf{w}_a \tag{6}$$

where $\ddot{z}$ is given by (2). The acceleration measurements do not go through a modal

decomposition process. These measurements are dependent on the modal frequencies and damping, values that are uncertain and will be estimated. Also, the accelerometers only produce a small amount of data at each time step compared to vision system.

Error covariance for the acceleration measurements is given by:

$$\Lambda_{w_a w_a} = \sigma_{w_a}^2 I_n \tag{7}$$

where $\sigma_{w_a}^2$ is the variance on the accelerometer measurements, and n is the number of accelerometers. It is assumed that all the accelerometers have equal measurement variance.

D. Kalman Filter

A Kalman filter is used to observe the coarse estimates of the modal coefficients obtained from the vision system and the acceleration measurements to obtain an estimate of $q_i(t)$ and $\dot{q}_i(t)$. The estimated state consists of the modal coefficients, their time derivatives, the natural frequencies, and the damping ratios. The continuous-time process model is given by:

$$\frac{d}{dt}\begin{Bmatrix} q_i \\ \dot{q}_i \\ \omega_i \\ \zeta_i \end{Bmatrix} = \begin{Bmatrix} \dot{q}_i \\ \sum_{k=1}^{p} b_{i,k} F_k - \omega_i^2 q_i - 2\zeta_i \omega_i \dot{q}_i \\ 0 \\ 0 \end{Bmatrix} \tag{8}$$

where $b_{i,k}$ is the magnitude of the mode shape φ_i at the position of the k^{th} robot. This continuous-time process model can be transformed into discrete-time by computing the matrix exponential. When expressed in discrete-time with time step Δ, the process model becomes:

$$\begin{Bmatrix} q_i \\ \dot{q}_i \\ \omega_i \\ \zeta_i \end{Bmatrix}_{(t+\Delta)} = \begin{Bmatrix} exp(-\zeta_i \omega_i \Delta) \cdot \left(q_i \cos(\omega_{d,i}\Delta) + \frac{\dot{q}_i + \zeta_i \omega_i q_i}{\omega_{d,i}} \sin(\omega_{d,i}\Delta) \right) \\ exp(-\zeta_i \omega_i \Delta) \cdot \left(\dot{q}_i \cos(\omega_{d,i}\Delta) - \frac{\zeta_i \omega_i \dot{q}_i + \omega_i^2 q_i}{\omega_{d,i}} \sin(\omega_{d,i}\Delta) \right) \\ \omega_i \\ \zeta_i \end{Bmatrix}_{(} + Force\ Term + v_i \tag{9}$$

The process noise is represented by $v \equiv \{v_q \quad v_{\dot{q}} \quad v_\omega \quad v_\zeta\}^T$ and it is characterized by the covariance matrix:

$$\Lambda_{vv} = E[vv^T] \tag{10}$$

The values of the entries in this matrix should be chosen to represent the uncertainty in the dynamic model.

The initial state estimate for this case is given by:

$$\{\hat{q}(0) \quad \hat{\dot{q}}(0) \quad \hat{\omega} \quad \hat{\zeta}\} = \{0 \quad 0 \quad \omega_{exp} \quad \zeta_{exp}\} \tag{11}$$

where the expected values for ω_{exp} and ζ_{exp} are calculated offline. The initial values of and are both set to zero since these values are unknown.

A modified Kalman filter is used to estimate the modal frequencies, modal damping, modal coefficients and their derivatives. Since the process model is non-linear, an unscented Kalman filter is used [18]. The filter is modified in order to accommodate the different sample rates associated with the accelerometers and vision sensors. There are two separate update models; the appropriate update model is applied based on the sensory information available at that time step, see Fig. 8.

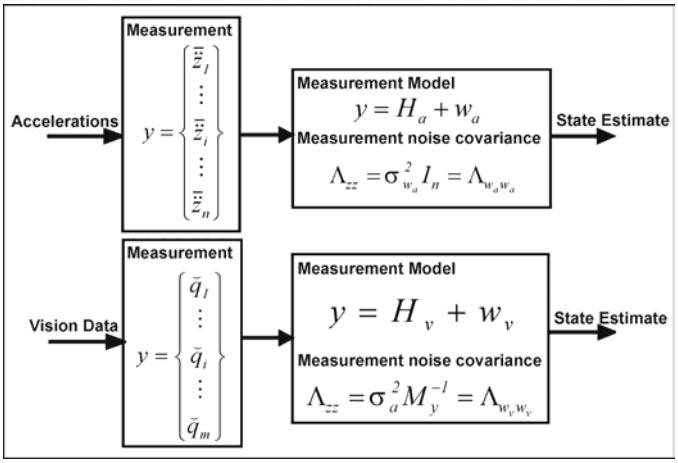

Fig. 8. Two measurement update models.

The vision-based measurements provide a coarse estimate of $q(t)$ to the Kalman filter. In this case the measurement model is given by:

$$\begin{Bmatrix} \breve{q}_1 \\ \vdots \\ \breve{q}_i \\ \vdots \\ \breve{q}_m \end{Bmatrix} = \begin{Bmatrix} q_1 \\ \vdots \\ q_i \\ \vdots \\ q_m \end{Bmatrix} + \begin{Bmatrix} w_{a1} \\ \vdots \\ w_{ai} \\ \vdots \\ w_{am} \end{Bmatrix} = H_v + w_v \tag{12}$$

The accelerometers provide acceleration measurements directly to the Kalman filter. The measurement model for the accelerometers is given by:

$$\begin{Bmatrix} \ddot{\tilde{z}}(x_1,t) \\ \vdots \\ \ddot{\tilde{z}}(x_k,t) \\ \vdots \\ \ddot{\tilde{z}}(x_n,t) \end{Bmatrix} = \begin{Bmatrix} \sum_{i=1}^{m}(b_{mi}F_{mp}(t)-\omega_i^2 q_i(t)-2\zeta_i\omega_i\dot{q}_i(t))\phi_i(x_1) \\ \vdots \\ \sum_{i=1}^{m}(b_{mi}F_{mp}(t)-\omega_i^2 q_i(t)-2\zeta_i\omega_i\dot{q}_i(t))\phi_i(x_k) \\ \vdots \\ \sum_{i=1}^{m}(b_{mi}F_{mp}(t)-\omega_i^2 q_i(t)-2\zeta_i\omega_i\dot{q}_i(t))\phi_i(x_n) \end{Bmatrix} + \begin{Bmatrix} e_{a1} \\ \vdots \\ e_{ak} \\ \vdots \\ e_{an} \end{Bmatrix} \quad (13)$$
$$= H_a + w_a$$

Implementation of this modified unscented Kalman filter is straightforward using (5-13) and applying the appropriate update as shown in Fig. 8.

E. Modal Reconstruction

In this final step, an estimate of the flexible structure's shape can be found using the knowledge of the mode shapes and the estimate of the modal coefficients. This reconstruction can be expressed as:

$$\hat{z}(x,t) = \sum_{i=1}^{m} \hat{q}_i(t)\phi_i(x) = \hat{\mathbf{q}}(t)^T \mathbf{\Phi}(x) \quad (14)$$

IV. Experimental Results

A series of experimental studies was conducted in the laboratory to determine if unmodeled effects degrade the performance of the estimator. The hardware for these experiments consisted of a granite surface plate, two floating modules, and a flexible structure.

The experimental setup is shown in Fig. 9. The granite surface plate serves as the base for the experimental system. The surface plate is 2.2 meters long by 1.3 meters wide and is finely levelled to simulate a two-dimensional microgravity environment. The floating modules were designed to operate on top of the micro-polished granite surface. These modules are supported by three low-friction, flat floatation bearings. The floatation bearings run on compressed carbon dioxide, which is stored on-board the modules. A flexible panel was mounted between two floating modules to simulate a one-dimensional space structure.

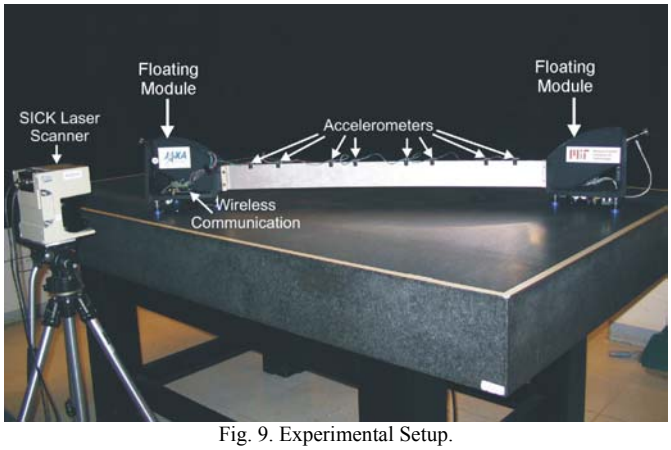

Fig. 9. Experimental Setup.

A simple beam structure was designed for the experiments. This structure is a thin beam made of stainless steel, which is clamped at each end to a floating module (see Fig. 9). The mode shapes and frequencies were computed using the FEM software ADINA. A summary of these properties is given in Table 2.

Table 2
Properties of Experimental Structure

Parameters	Values
Material	Stainless Steel
Dimensions	Flexible Beam - 1000mm long, 80mm tall, 0.76mm wide
Flexural Rigidity	560 x 10^{-6} Nm^2
Mass	6.5 kg Tanks Full, 5.6 kg Tanks Empty
Natural Frequencies	0.82Hz, 2.07Hz, 5.03Hz, 9.59Hz

The flexible structure is equipped with eight accelerometers manufactured by Analog Devices. The accelerometers were placed using the D-Optimality criteria [18]. These accelerometers have a measurement range of +/- 1.2g and a measurement variance (σ_a^2) of 0.013g^2. The accelerometers are sampled at a rate of 267 Hz. These values are then transmitted wirelessly to a ground computer system and are logged for post-processing.

A SICK LMS 291 laser scanner is mounted on a tripod next to the air table to provide the vision deflection measurements of the flexible structure. This system is able to capture 75 sweeps per second at an angular resolution of 1 degree. Like any laser measurement system, the measurements are noisy, and regions of structure may be unmeasureable due to limited reflectivity. The measurement variance in the range direction (σ_v^2) for this system was observed to be 1.7mm^2.

A camera, made by Videre Design, is mounted above the granite table to observe the structure and

provide a ground-truth of its motion. This overhead camera collected images at a rate of 15 Hz. Software processed the images in real-time in order to track seven points on the vibrating structure. These measurements had a resolution of 6mm. Note that this information is not used by the estimator, it is just used to compare results.

Structural vibrations are induced manually. The structure is deformed and then carefully released in order to minimize any translation or rotational motion. It is necessary to reduce these motions to ensure the structure will remain vibrating on the table long enough to allow the estimator to converge. Once the structure has been released the data collection begins. All of the measurements are time-stamped to ensure the different measurements will be coordinated.

The experimental data was analyzed offline. This analysis varied two parameters: the number of accelerometers used in the estimation and the sample rate of the vision sensor. The number of accelerometers and the vision sample rate were varied by ignoring the appropriate measurements.

The RMS error in the shape estimate at the 7 points tracked by the overhead camera is used to compare the different sensor configurations. The shape estimate neglects rigid body motion. Here, the comparison metric is the time required for the RMS error to converge within 2.4 cm (4 pixels of the overhead system) of the ground truth. We placed the artificial specification that this must happen within 10 seconds.

Ten different sets of experimental data were analyzed. The first vibrational mode was dominant in 5 of the data sets, and the second vibrational mode was dominant in the other 5 data sets. A total of 4 modes were estimated.

Fig. 10 shows how the convergence rate varies for estimates using only measurements from the SICK laser scanner. Estimates using vision data at a sample rate below 4.5 Hz are unable to converge within the timeframe of the experiment. The estimate is only able to meet the desired specification when the sample rate is 28 Hz or higher. This sample rate may be too high for real-time implementation of the estimator.

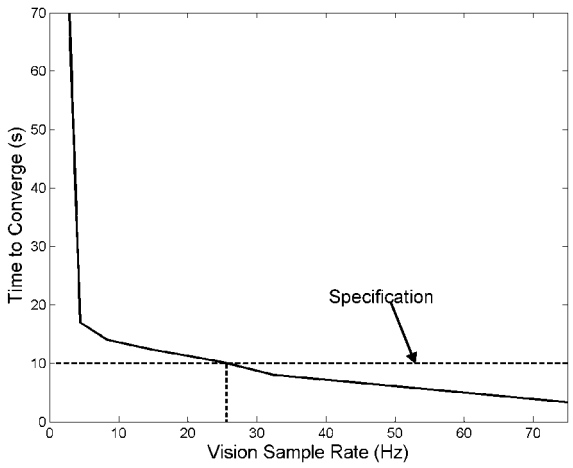

Fig. 10. Convergence of vision based estimates.

Fig. 11 shows the shape estimate at a point on the structure using 9 Hz vision data. Nine Hz is a reasonable rate for online implementation of this system. The estimator a does good job estimating the phase of the vibration, but it is unable to converge to the correct amplitude within the specified time.

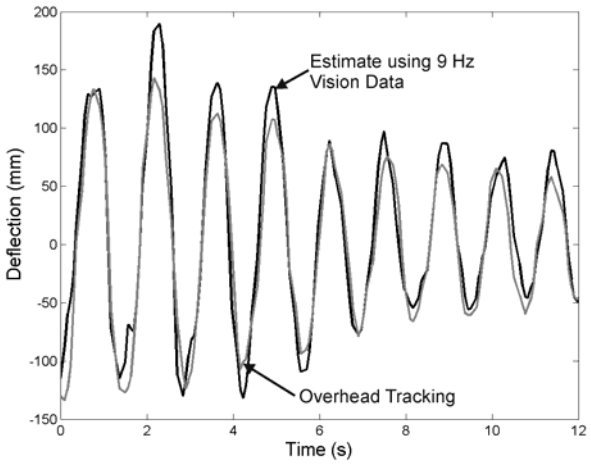

Fig. 11. Deflection of a point 8 cm along the structure using a estimate from 9-Hz vision data.

Fig. 12 shows the estimate formed by 9-Hz vision data compared with the ground truth measurements. The circles represent the 7 points tracked by the overhead camera. As stated above, the estimator is able to match the phase of the vibration but is unable to converge to the proper amplitude. Fig. 13 shows the RMS error of the vibrational motion for this configuration. The estimate is unable to converge to within the desired tolerance within 10 seconds.

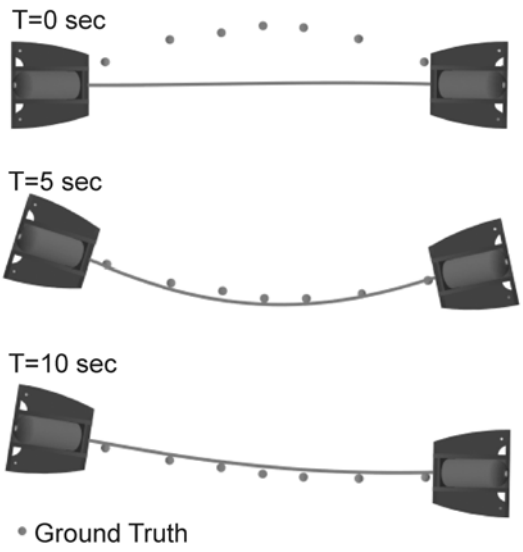

Fig. 12. Estimate from 9-Hz vision data.

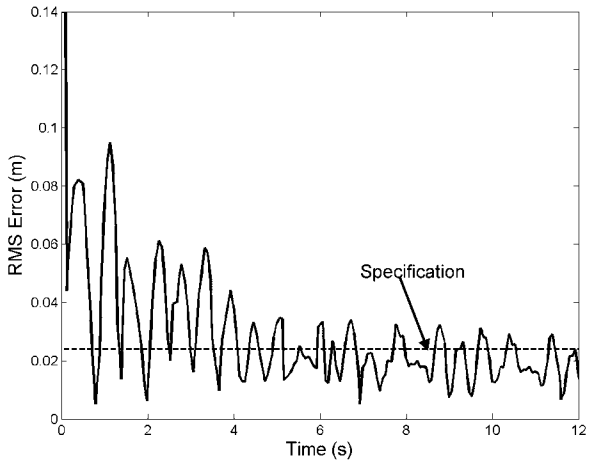

Fig. 13. RMS error of an estimate using 9 Hz vision data.

Fig. 14 shows how the convergence rate varies for estimates using only measurements from the accelerometers. Estimates formed using 1 accelerometer are unable to converge during the length of an experimental trial. The estimate is only able to meet the desired specification when 6 or more accelerometers are used. This is an unreasonable number for such a simple structure. For a larger, more complex structure many more accelerometers would be required. It should also be noted that rigid-body motions cannot be estimated with only accelerometers.

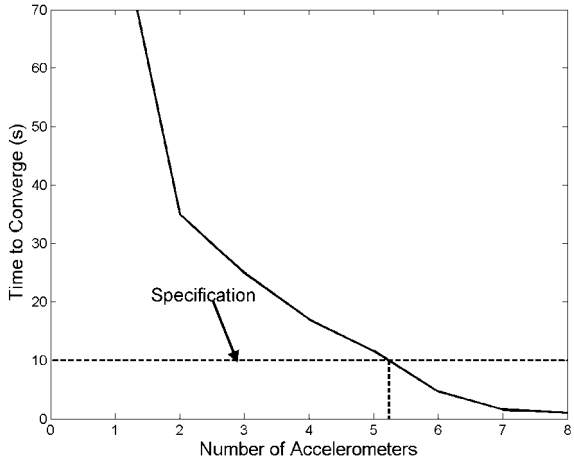

Fig. 14. Convergence of acceleration-based estimates.

Fig. 15 shows the shape estimate at a point on the structure using data from 3 accelerometers. Three accelerometers are a reasonable number for a structure of this size. The estimator converges to the proper phase but is unable to reach the appropriate amplitude in the specified amount of time.

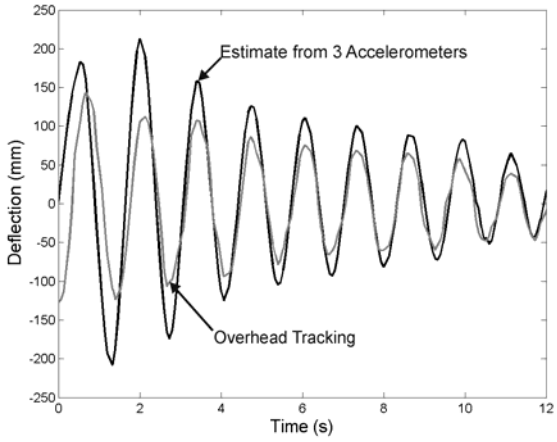

Fig. 15. Tracking of a point 8 cm along the structure using an estimate from 3 accelerometers.

Fig. 16 shows the estimate formed by 3 accelerometers compared with the ground truth measurements. The circles represent the 7 points tracked by the overhead camera. The estimator is unable to track the rigid-body motion but is able to match the phase of the vibration. Fig. 17 shows the RMS error of the vibrational motion for this configuration. The estimate is unable to converge within 10 seconds.

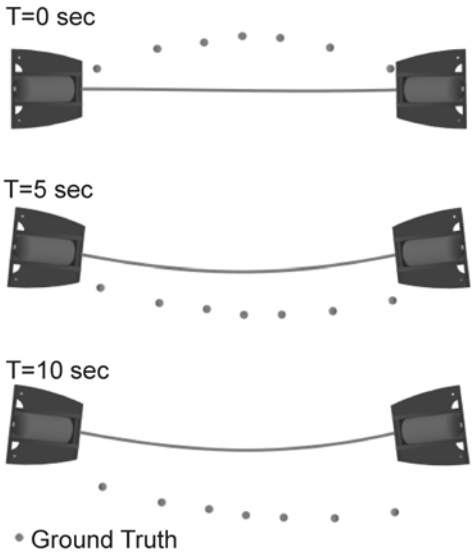

Fig. 16. Estimate from 3 structure-mounted accelerometers.

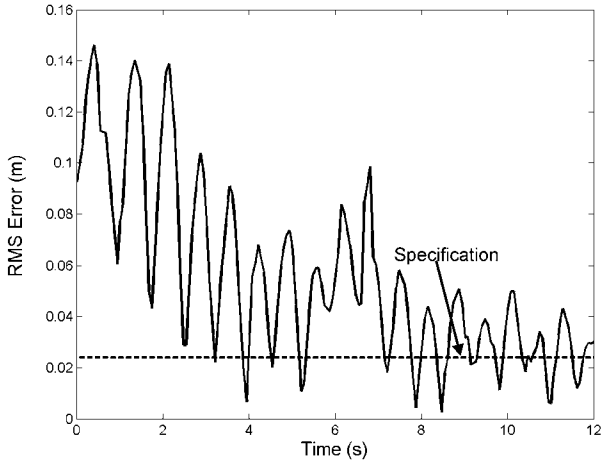

Fig. 17. RMS error of an estimate using 3 accelerometers.

Fig. 18 shows a range of sensor configurations that meet the specification. One configuration that meets the specifications uses 3 accelerometers and a vision sample rate of 9 Hz. This is a reasonable configuration for real-time implementation of this system.

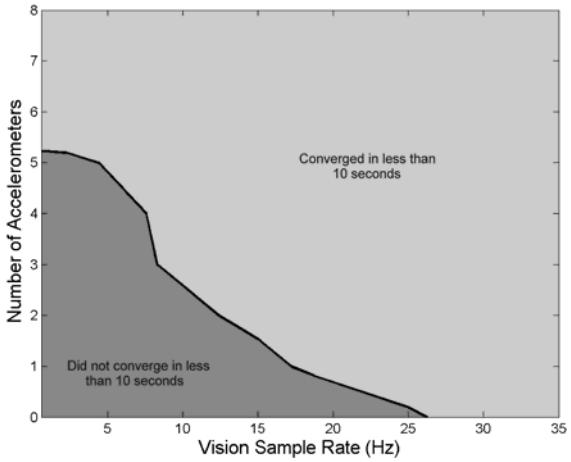

Fig. 18. Sensor configurations, experimental results.

One configuration that meets the desired specifications is 3 accelerometers and 9-Hz vision data. Fig. 19 shows the shape estimate at a point on the structure for this configuration. After 5 seconds, the deflection measured by the overhead camera and the estimated deflection are nearly identical.

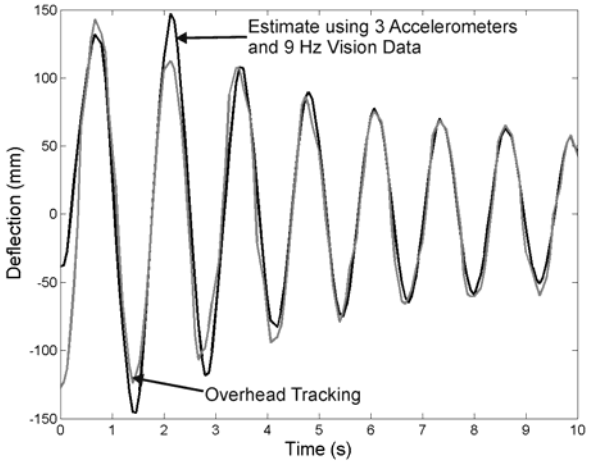

Fig. 19. Tracking of a point 8 cm along the structure using an estimate from 3 accelerometers and 9 Hz vision data.

Fig. 20 shows the estimate formed by 3 accelerometers and 9-Hz vision data compared with the ground truth measurements. The estimate matches the ground-truth almost identically after 5 seconds. Fig. 21 shows the RMS error of the vibrational motion for this configuration. The estimate is able to converge to within the desired tolerance within 7.5 seconds. This configuration meets the specifications.

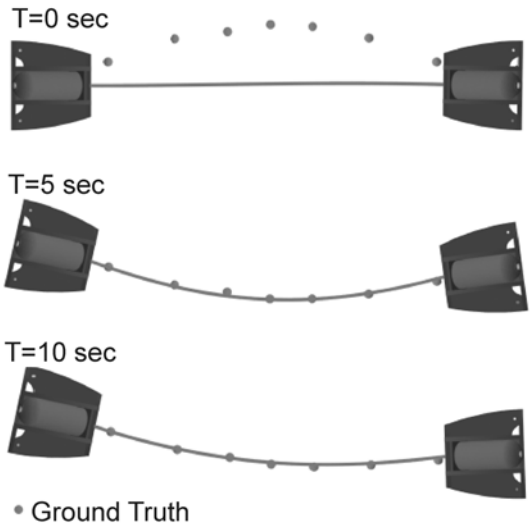

Fig. 20. Estimate from 3 structure-mounted accelerometers and 9-Hz vision data.

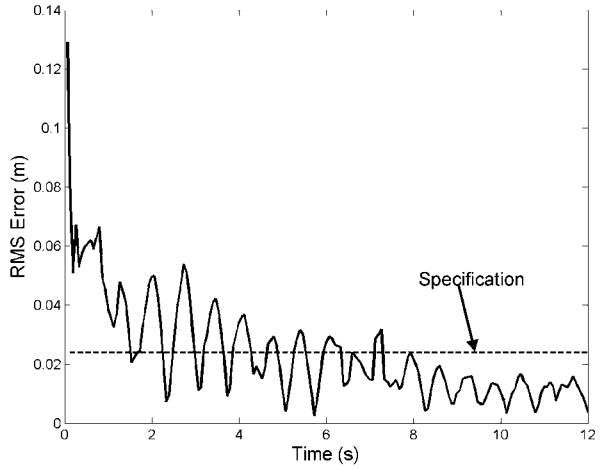

Fig. 21. RMS error of an estimate using 3 accelerometers and 9 Hz vision data.

Work is currently underway to experimentally verify the decoupled LSS transportation controller presented in Section II. In order to complete this experiment, two free-flying robotic agents have been constructed. Each robotic agent is equipped with 2 manipulators and has 8 cold-gas thrusters to propel itself around the granite table. In addition, each robot is equipped with wireless ethernet to allow communication with other robots and remote sensors. The setup for this experiment is shown in Fig. 22.

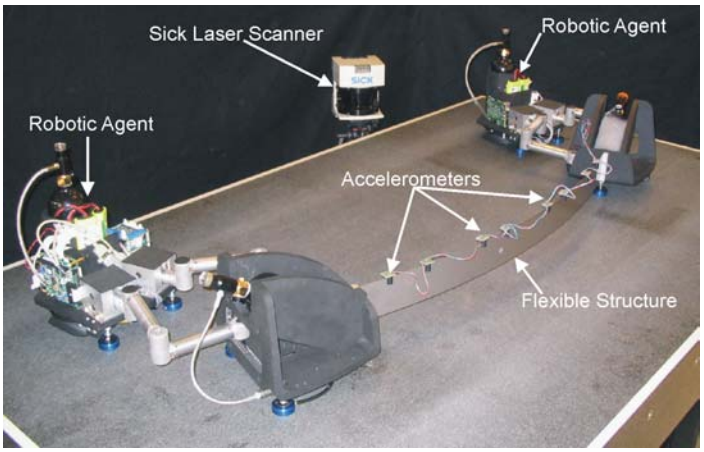

Fig. 22. Setup for LSS transportation experiment.

V. Summary and Conclusions

This paper develops a sensor architecture for the vibration estimation of a flexible space structure. It combines measurements from high-frequency accelerometers and a low-frequency vision system using a modified unscented Kalman filter to obtain an estimate of the flexible structures shape. This estimator can be used in the feedback loop of an active modal damping controller. The performance of this fusion-based estimation approach was tested experimentally. In these experiments, it was shown that vision and acceleration-based estimator was able to meet the performance specification with a limited number of on-board acceleration sensors and relatively low vision system sample rate.

Acknowledgements

The authors would like to thank the Japan Aerospace Exploration Agency (JAXA) for their support of this research, as well as Dr. Yoshiyuki Okhami, Dr. Mitsushige Oda, Mr. Hiroshi Ueno, and Dr. Karl Iagnemma for their helpful comments during the development of this work.

References

[1] Staritz, P.J., S. Skaff, C. Urmson, and W. Whittaker. "Skyworker: A Robot for Assembly, Inspection and Maintenance of Large Scale Orbital Facilities." *Proc. 2001 IEEE Int. Conf. on Robotics and Automation (ICRA 2001)*, Seoul, Korea, pp. 4180-4185, May 2001.

[2] Oda, M., H. Ueno, and M. Mori. "Study of the Solar Power Satellite in NASDA." *Proc. 7th Int. Symp. on Artificial Intelligence, Robotics, and Automation in Space: i-SAIRAS 2003*, NARA, Japan, May 2003.

[3] Ishijima, Y., D. Tzeranis, and S. Dubowsky. "On-Orbit Maneuvering of Large Space Flexible Structures by

Free-Flying Robots." *8th International Symposium on Artificial Intelligence, Robotics and Automation in Space, i-SAIRAS*, Munich, Germany, September 2005.

[4] Ueno, H., T. Nishimaki, M. Oda, and N. Inaba. "Autonomous Cooperative Robots for Space Structure Assembly and Maintenance." *Proceedings of the 7th International Symposium on Artificial Intelligence, Robotics, and Automation in Space: i-SAIRAS 2003*, NARA, Japan, May 2003.

[5] Chen C.-W., Huang, J.-K., Phan, M. and J.-N. Juang, "Integrated system identification and state estimation for control of flexible space structures." Journal of Guidance, Control and Dynamics, Vol. **15,** No. **I ,** p. 88 – 95, Jan-Feb 1992.

[6] Williams, T. and G. Slater, "Steady-State Matched Model Reduction for Flexible Structures with Acceleration Measurements." Journal of Guidance, Control, and Dynamics, Vol. 28, No. 2, p. 360-363, March-April 2005.

[7] Balas, G. J., and J. C. Doyle, "Identification of Flexible Structures for Robust Control." IEEE Control Systems Magazine, p. 51-58, June 1990.

[8] Zhang, H.-H. and H.-X. Wu. "Identifiability of Flexible Space Structures." *Proc. IEEE Conf. on Decision and Control*, Vol. 2, pp. 1488-1493, Dec. 1993.

[9] Maghami, P.G. and S.M. Joshi. "Sensor/Actuator Placement for Flexible Space Structures." *IEEE Trans. on Aerospace and Electronic Systems*, Vol. 29, No. 2, pp. 345-351, April 1993.

[10] Lichter, M.D., S. Dubowsky, H. Ueno, and S. Mitani. "Shape, Motion and Parameter Estimation of Flexible Space Structures using Laser Range Finders," *Proceedings of Robotics: Science and Systems*, Cambridge, MA, June 2005.

[11] Lichter, M.D. "Shape, Motion, and Inertial Parameter Estimation of Space Objects using Teams of Cooperative Vision Sensors." PhD Thesis, Dept. of Mech. Eng., MIT, Sept. 2004.

[12] Tse, D. N. C. and G. R. Heppler. "Shape Determination for Large Flexible Satellites via Stereo Vision," *Journal of Spacecraft and Rockets*, Vol. 29, No. 1, pp. 108-117, 1992.

[13] Bayard, B. S., F. Y. Hadaegh, and D. R. Meldrum. "Optimal Experiment Design for Identification of Large Space Structures," *Automatica*, Vol. 24, No. 3, pp. 357-364, 1998.

[14] Bilton, A.M. "Fusion of Remote Vision and On-Board Acceleration Data for the Vibration Estimation of Large Space Structures." M.S. Thesis, Dept. of Aeronautics and Astronautics, MIT, June 2006.

[15] Lim, K.B., P.G. Maghami, and S.M Joshi. "Comparison of Controller Designs for an Experimental Flexible Structure." *IEEE Control Systems Magazine,* vol. 12, no. 3, pp. 108–118, June 1992.

[16] Kar, I.N., K. Seto, and F. Doi. "Multimode Vibration Control of a Flexible Structure Using H_∞-Based Robust Control." *IEEE/ASME Transactions on Mechatronics*, vol. 5, no. 1, March 2000.

[17] Bostelman, R., J. Albus, N. Dagalakis, A. Jacoff, and J. Gross, "Applications of the NIST RoboCrane." *5th International Symposium on Robotics and Manufacturing*, Maui, HI, August 1994.

[18] Julier, S.J., and J.K. Uhlmann. "A New Extension of the Kalman Filter to Nonlinear Systems." *Proc. AeroSense: The 11th Int. Symp. on Aerospace Defense Sensing, Simulation and Controls*, Orlando, Florida, 1997.